1999-01-0094

Practical Analysis Technique for Quantifying Sideswipe Collisions

Amrit Toor, Eric Roenitz, Ravinder Johal, Robert Overgaard, Andrew Happer and Michael Araszewski
INTECH Engineering Ltd.

ABSTRACT

This paper presents a practical analytical approach for evaluating sideswipe collision severity from residual vehicular deformation. A simplified mathematical procedure was developed to evaluate vehicular speed changes, effective average vehicular acceleration rates and the collision duration from measurements of vehicular damage.

Several series of sideswipe collisions were staged to acquire empirical sliding contact data. The results of this testing were employed to provide a preliminary validation of the proposed analysis model. The limited validation supported the use of the proposed analysis technique to assess a vehicle's speed change resulting from a sideswipe collision.

INTRODUCTION

Vehicular collisions in which the surface of one vehicle slides against another vehicle or object are often colloquially termed as "sideswipe" collisions. In "conventional" vehicular impacts, the collisions are characterized by sudden speed changes in which the interacting surfaces achieve a common velocity. Conversely, in a sideswipe collision, the two contact surfaces do not necessarily achieve a common velocity. The sideswipe collision duration may range from relatively short (i.e. <0.05 seconds) to relatively long (i.e. >1 second) depending on the circumstances.

Collision analysts are often retained to evaluate the circumstances of a sideswipe collision; as part of this investigation it is typically necessary to determine the collision severity. The residual vehicular damage sustained by the involved vehicle(s) may be the only physical evidence remaining after the collision. Therefore, there is a need for a practical method to analyze sideswipe collisions from the vehicular damage.

Due to the combination of perpendicular and frictional forces acting during a sideswipe collision and the difficulty in interpreting vehicular damage patterns, this class of collisions is often difficult to analyze. As such, a standardized and practical analysis technique for evaluating this class of automobile collisions has not emerged. This paper presents a practical approach for analyzing sideswipe collisions from the residual vehicular damage. A series of sideswipe collisions were staged using monitored test vehicles; data collected from this testing were employed to conduct a preliminary validation of the proposed analytical model.

THE SIDESWIPE COLLISION

Sliding contact collisions may occur between two vehicles or between a vehicle and a stationary object. For the purpose of discussion and ease of exploration, sideswipe collisions involving two vehicles will be described. There are two general classifications for the vehicles involved in a sideswipe collision. Vehicles that exhibit evidence of sliding contact over extended lengths are designated as "surface" vehicles; this descriptor reflects contact across an extended surface. Vehicles that exhibit evidence of sliding contact over localized regions are designated as "contact" vehicles; this descriptor reflects contact to a relatively localized area. In this paper, the surface vehicle is designated as vehicle A; variables denoted with subscript "A" refer to the surface vehicle. Correspondingly, the contact vehicle is designated as Vehicle B; variables denoted with subscript "B" are specific to the contact vehicle.

If the corner of one vehicle's bumper slides along the side of another vehicle, then the vehicle with bumper damage is the contact vehicle and the vehicle with the side panel damage is the surface vehicle. Figure 1 illustrates three common geometries for sideswipe collisions. The two vehicles on the far right illustrate a collision scenario in which both vehicles sustain extended contact surfaces and are both designated as surface vehicles. Sideswipe collisions can occur with two surface vehicles but they cannot occur with two contact vehicles since a sideswipe collision involves prolonged sliding contact.

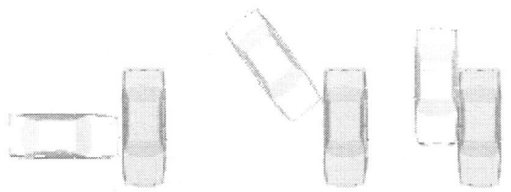

Figure 1. Typical Sideswipe Impact Geometries

Sliding contact interactions are complex events involving multiple applications of force and extended regions of contact. An automobile being contacted has lateral tire reaction forces acting with the ground surface plus longitudinal tire traction forces if the vehicle is braking or accelerating. During a sideswipe, the force applied to the surface of a vehicle can be resolved into a normal component acting perpendicular to the surface and a frictional component acting along its surface. As the sliding progresses, the point of force application advances across the contacted area. Depending on the circumstances, there may be sufficient applied force to rotate the involved vehicle in the plane parallel with the road surface. An additional complexity arises in that vehicles are not rigid bodies, but are actively coupled to the tires via a damped elastic suspension. Forces applied to the side of a vehicle may cause the body to shift laterally as the vehicle's weight is redistributed on the four tires.

SCOPE OF PROJECT

This paper is intended to present a practical procedure for evaluating the average acceleration rate and total vehicular speed change sustained during a sideswipe collision. The following criteria define the scope of this analysis:

- Sliding contacts sometimes involve snagging of the two interacting surfaces. A snag may be recognized as a point on the side of a vehicle that is deformed rearward or forward; pure sliding contact is observed as abrasions or scuff marks with inward deformation of the body skin. As snagging and sliding contact are differing vehicular contact mechanisms, snagging is not considered within this paper. In those cases where snagging occurs in combination with sliding contact, the forces developed during each of these two mechanisms should be independently considered in the reconstruction of the accident.
- The presented procedure has been derived for the collision between vehicles that are not braking or accelerating.
- This analytical model is intended for application to sideswipe collisions where the inward crush of the contacted vehicular surfaces does not exceed about 4 cm; the referenced coefficients of friction may not be applicable outside of this range.
- This methodology is directed for application to vehicles that do not experience large rotation due to the collision forces. Large vehicle rotations would not be expected to occur during sideswipe collisions that satisfy the preceding qualifications; this statement is supported by the observation that significant vehicular rotation did not occur in the conducted tests that are presented later in this paper. However, collisions occurring on very low friction surfaces (eg. ice) may permit greater vehicle rotation and violate this requirement.
- This analysis considers the front tires of all vehicles to be steered straight forward.

The previous points outline the intended limits of this analysis procedure in its presented form. However, the technique presented in this paper may be adapted to incorporate the necessary factors for collision scenarios that are outside of these bounds. Within the defined scope, three assumptions may be applied to reduce the complexity of the sideswipe collision reconstruction:

- The sides of each vehicle are assumed to be straight and parallel to the vehicle's midline. Therefore, a force that is perpendicular to the side of a vehicle is parallel to the vehicle's axles and the corresponding frictional force component is parallel with the free rolling direction of its tires. For vehicle geometries where this assumption is invalid, it is necessary to resolve the collision forces into their components acting parallel and perpendicular to the vehicle's midline before proceeding through the analysis.
- The involved vehicles are considered to act as rigid bodies in this analysis; body motion on the vehicles' suspensions and lateral flexing of the tire sidewalls are ignored. This simplification may be justified with the recognition that the vehicle motion relating to these two mechanisms is limited.
- Free rolling (i.e. not braking or accelerating) vehicle tires are assumed to have negligible rolling resistance as the rolling resistance of automobile tires is typically about 0.01g [3]

REVIEW OF LITERATURE

SIDESWIPE COLLISIONS – A review of available literature yielded no practical technique for analyzing sideswipe collisions. The majority of reviewed papers concentrate on front or rear impacts; these sources mention, but do not explore, inter-vehicular sliding contact. Among those sources that reference side impacts, the focus is on high speed collisions. However, a paper by Bailey, et al.[1] addresses the analysis of sideswipe collisions.

Bailey, et al. proposed an innovative approach for quantifying the magnitude of sliding contacts. It was proposed that the severity of sideswipe collisions may be quantified in terms of the Vibrational Dose Value (VDV). The VDV was previously addressed in a 1986 paper by Griffin[2]

where the relationship between this vibrational index and the occurrence of motion sickness was being explored. The VDV is defined as :

$$VDV = \sqrt[4]{\int_{t_1}^{t_2} a^4 \, dt} \qquad (1)$$

where a = acceleration

t = time

The basis of the VDV relationship is that injury to vehicle occupants is generally caused by an oscillating acceleration. Since the VDV weights its integral to magnify the effect of the peak accelerations, it was proposed to be a valid measure of the collision severity from the perspective of injury causation.

The Bailey, et al. paper presents experimental results which suggest that the VDV can be correlated to the severity of a rear end impact. Sideswipe tests were also conducted; the tabulated data for the sideswipe tests do not support a high degree of correlation with the VDV.

Estimation of the VDV sustained by a vehicle by comparing damage profiles yields uncertain results because similar damage profiles may be produced by accident scenarios with a wide range of collision time durations. As the duration of contact is highly influential in the assessment of the total resultant speed change, this ambiguity requires significant subjective input by the examiner to apply the VDV method to a real world collision. Furthermore, although it is relatively simple to assess the VDV sustained by an instrumented test vehicle, the evaluation of the VDV for real world collisions is problematic. A practical methodology for applying the VDV technique in real world applications is not proposed in the Bailey, et al. paper.

INTER-VEHICULAR FRICTION COEFFICIENT – Evaluation of the inter-vehicular frictional forces developed in a sideswipe collision requires application of a vehicle-to-vehicle friction coefficient. Several sources of friction data exist. Warner, et al.[3] tabulates a "car-to-car" coefficient of friction of 0.55 and a "body sheet metal on body sheet metal (sideswipe)" coefficient of friction of 0.6. The Warner paper references the "car-to-car" coefficient of friction to the prior work of Emori[4]. However, the Emori paper presents the coefficient of friction between two vehicles to be 0.36.

These coefficients are presented to be applicable for sliding contact between the sides of two vehicles. As vehicle body exteriors are typically painted, it is logical to widely apply these values for contact between painted metallic vehicle surfaces. However, with the increasing use of alternative automotive construction materials, these coefficients of friction may not be representative for all vehicle contacts. Inter-vehicular contacts involving structures other than body sheet metal (eg. an unpainted plastic bumper molding) require appropriate selection of a coefficient of friction specific to the contacting materials.

An inter-vehicular coefficient of friction of 0.6 is assumed to be representative for the tests documented within this paper.

In the case of inter-vehicular "snagging" (the interlocking of surfaces or structures between the vehicles' contacting areas), the effective friction coefficient can be much higher than the referenced value of 0.6. The scope of this paper does not include the establishment of an effective coefficient of friction for the phases of vehicular collisions which involve snagging.

ANALYTICAL MODEL FOR SIDESWIPE COLLISIONS

The proposed analytical model provides a technique for evaluating the severity of a sideswipe collision from residual deformation. This model utilizes the principles of the Crash 3 analysis algorithm (commonly used to analyze lateral, frontal and rear impacts) and empirically derived vehicle stiffness coefficients to ultimately determine the average acceleration rate and total speed change of each vehicle. However, several other parameters must be assessed as intermediate steps in the analysis:

1. Contact forces
2. Longitudinal acceleration rates
3. Relative sliding distance
4. Contact duration

It is cautioned that these parameters are intermediate steps in the analysis and their values may be potentially misleading if applied outside of their intended context.

This model is presented for a collision between two vehicles. However, the analysis technique can also be applied for a single vehicle sideswipe collision involving an inanimate object such as a tree or pole. A worked example of the complete analytical process in both metric and imperial units follows in Appendix A.

CHOICE OF COORDINATE SYSTEM – The coordinate grid for the vehicle-to-vehicle system may be selected at the discretion of the analyst; however, as the collision parameters are primarily calculated for the surface vehicle, the coordinate system utilized in this paper will be defined with the "longitudinal" axis parallel and the "lateral" axis perpendicular to the surface vehicle's longitudinal midline.

The contact forces acting on the contact vehicle may be more conveniently resolved into a coordinate system based upon the contact vehicle, and then translated into the surface vehicle's system coordinates. It is common for the striking vehicle to be contacted at a corner; in such a circumstance, it should be recognized that the direction of normal and frictional forces on the contact vehicle may not align with its longitudinal or lateral axes.

CONTACT FORCES – Newton's laws of motion state that an object will accelerate in the direction of the net applied force at a magnitude equivalent to the net force divided by mass. Therefore, the contact forces acting on the surface vehicle must first be assessed in order to determine the vehicle's net acceleration.

The normal force (F_n) is defined as the perpendicular force applied to the surface vehicle. This force may be evaluated by a variety of techniques, depending on the types of structures that are in contact. One technique for evaluating this perpendicular force from residual damage utilizes the Crash 3 force model. Over a specific contact width (C) acting on the surface vehicle, this algorithm stipulates that exterior deformation does not occur until a threshold force per unit length (A) is applied. Any additional force will then crush the surface of the vehicle with the force magnitude directly proportional (proportionality factor of B) to the depth of crush (x).

$$F_n = C(A + Bx) \qquad (2)$$

The A and B stiffness coefficients have historically been tabulated in imperial units of lb/in and lb/in^2, respectively. Vehicle specific stiffness coefficients are derived from empirical testing and are available in published literature [5,6,7]. For the sideswipe collisions considered in this paper, the normal force typically has a greater dependance on the A stiffness coefficient than the B stiffness coefficient. The length of the contact patch (C) acting on the surface vehicle is given by the width of contact measured on the contact vehicle.

The analytical model presented in this paper evaluates the total speed change from the average vehicle acceleration and the sliding duration. The average acceleration is directly proportional to the net force experienced by the surface vehicle. Furthermore, the applied force is linearly proportional to the crush depth (x) by the relationship presented in equation 2. Therefore, it is convenient to perform the averaging process at this stage by defining "x" as the average crush depth across the contact length on the surface vehicle. The average normal force (F_n) acting on the surface vehicle is then given by equation 2.

The frictional force (F_f) is defined as the sliding force acting between the contact areas of the vehicles. The frictional force may be evaluated directly from the normal force (F_n) by:

$$F_f = \mu_v F_n \qquad (3)$$

Inter-vehicular coefficient of friction (μ_v) values were presented in the review of relevant literature. It was reported that a coefficient of 0.6[3] is applicable to "body sheet metal on body sheet metal (sideswipe)" contacts. Consequently, this value was assumed to be representative for this study. However, further research may refine the coefficient of friction values applicable to vehicle-to-vehicle sliding interaction.

LONGITUDINAL ACCELERATION – The determination of the surface vehicle's net acceleration requires consideration of all external forces acting on the vehicle. If the surface vehicle's tires are free rolling, then the longitudinal component of acceleration ($a_{A\text{-}long}$) is dependent on the frictional contact force (F_f) and the vehicle's mass (m_A) as given by Newton's second law of motion:

$$a_{A-long} = \frac{F_f}{m_A} \qquad (4)$$

Assessment of the corresponding acceleration rate ($a_{B\text{-}long}$) of the contacted area on the contact vehicle along the surface vehicle's longitudinal axis requires consideration of the applied forces, tire traction and relative vehicular orientation. The assessment of this acceleration rate ($a_{B\text{-}long}$) is outlined in Appendix B.

RELATIVE SLIDING DISTANCE – Unlike the damage profile produced during "conventional" impacts, the damage profile produced during sliding contact is not produced simultaneously. Since inter-vehicular forces can only be transferred through the areas of direct interaction, the damage observed on the surface vehicle is produced as an area on the contact vehicle slides along the surface vehicle.

At the onset of the sideswipe collision, the contact vehicle's contact patch (of width C) engages the surface vehicle. This contact patch then slides along the surface vehicle recording evidence of contact over the measured length (L). The effective relative distance (D) traveled by the contact vehicle with respect to the surface vehicle during this sliding process may be interpreted from the vehicular damage.

In some collisions, the interaction of the involved vehicles may involve the full width of the contact patch instantaneously engaging and disengaging at the ends of contact; in this circumstance, a constant contact width acts for the full duration of contact. In other collisions, the interaction between the involved vehicles may gradually engage and disengage at the ends of the sideswiped region. The effect of these transition periods is to maximize the relative distance traveled between the vehicles during the sliding process. However, the contact forces acting during the transitions are reduced. These two factors oppose each other and result in an effective relative distance (D) that is likely comparable to the constant width contact patch case. The distance slid by a constant width contact patch during a sideswipe event is given by:

$$D = L - C \qquad (5)$$

CONTACT DURATION – "Conventional" impacts typically result in the contacting surfaces interlocking and remaining in direct contact for the duration of the collision. In such cases, the contacting surfaces do not appreciably move with respect to each other for the duration of contact, and these surfaces are designated as achieving a "common velocity". In sideswipe collisions, the contact surfaces slide against each other and may not attain a common velocity at the end of sliding contact.

For sideswipe collisions in which the interacting surfaces do not reach a common velocity at the end of sliding contact, the initial or final closing speed (V_c)* along the longitudinal axis of the surface vehicle must be known to assess the collision duration. If neither of these closing speeds is known, then a maximum estimate of the collision duration may be evaluated by assuming that the contacting surfaces attain a common velocity at the end of sliding contact; this maximum duration will ultimately yield a maximum estimate of the speed change.

The closing speed (V_c) along the sliding surface may also be conceptualized as the sliding speed; the closing speed corresponds to the relative difference in speed between the interacting surfaces. For surface vehicle A sliding on contact vehicle B, the longitudinal closing speed ($V_{c\text{-}long}$) may be calculated from the vector difference in speed components ($V_{A\text{-}long}$ and $V_{B\text{-}long}$, respectively) along the longitudinal axis of the surface vehicle:

$$V_{c-long} = \left| V_{A-long} - V_{B-long} \right| \qquad (6)$$

A related expression is the closing acceleration rate (a_c); the closing acceleration rate is defined as the change in the closing speed (V_c) during the inter-vehicular interaction, and is given by the vector difference between the acceleration rate components ($a_{A\text{-}long}$, and $a_{B\text{-}long}$, respectively) of vehicles A and B along the longitudinal axis of the surface vehicle. Since the accelerations of the vehicles will be in opposite directions the closing acceleration can be calculated from:

$$a_c = \left| a_{A-long} \right| + \left| a_{B-long} \right| \qquad (7)$$

Expressions for the contact duration (Δt) may be developed by applying elementary calculus:

$$D = \int_0^t V_c \, dt$$

$$D = V_{c-initial} \Delta t - \frac{1}{2} a_c (\Delta t)^2 \qquad (8)$$

where: $V_{c-initial}$ = the closing speed at the initiation of contact.

Solving equation 8 yields an expression to calculate the collision duration (Δt) when an estimate of the initial closing speed ($V_{c\text{-initial}}$) is available:

$$\Delta t = \frac{V_{c-initial} - \sqrt{V_{c-initial}^{\ 2} - 2 * a_c * D}}{a_c} \qquad (9)$$

If the final closing speed ($V_{c\text{-final}}$) is known or can be assessed from post-collision vehicle events, then the collision duration may be evaluated from:

$$\Delta t = \frac{-V_{c-final} + \sqrt{V_{c-final}^{\ 2} + 2 * a_c * D}}{a_c} \qquad (10)$$

The maximum collision duration occurs if the vehicles reach a common velocity at the end of the sideswipe (i.e. $V_{c\text{-final}}=0$). If it is known that the contacting surfaces of the vehicles attained a common velocity at the end of sliding contact, then the contact duration corresponds to this maximum case and may be directly assessed. Additionally, for collisions where there is insufficient information to estimate the initial closing speed or the final closing speed, then the maximum theoretical collision duration may be calculated by assuming that the vehicles achieve a common velocity at the end of contact. The maximum contact time (Δt_{max}) value is defined by the equation:

$$\Delta t_{max} = \sqrt{\frac{2 * D}{a_c}} \qquad (11)$$

Thus, the total sideswipe duration is defined by equation 9, 10 or 11, depending on the collision circumstances and available information.

LONGITUDINAL SPEED CHANGE – The longitudinal speed change ($\Delta V_{A\text{-long}}$) of the surface vehicle due to the sliding contact can be determined from the calculated collision duration:

$$\Delta V_{A-long} = a_{A-long} \Delta t \qquad (12)$$

where: Δt is given by equation 9, 10 or 11, depending on the collision circumstances

* Closing Speed: The closing speed is the speed at which the vehicles are approaching each other. The closing speed decreases during the collision as the vehicles approach a common velocity.

If the closing speed is unknown and a maximum theoretical contact time (Δt_{max}) is used in equation 12, then this analysis will yield a maximum estimate of the speed change.

LATERAL SPEED CHANGE – If the net lateral force acting on the surface vehicle is sufficient to overcome the reaction forces at the tires, then the vehicle will be displaced laterally. It should be noted that a lateral force may also cause the vehicle body to minorly shift laterally as compliance in the suspension and tire sidewalls permits a limited degree of lateral motion. These body roll motions are not considered within this analysis; this analysis evaluates the net displacement of the entire vehicle system.

Each tire supports a portion of the automobile's weight and generates a proportional amount of traction with the ground. The lateral tire traction force vectors generated by the rear pair of tires are collinear. Consequently, the rear tire traction forces may be mathematically represented as a single lateral force acting through the rear axle at its midpoint. Similarly, with the front tires steered straight, the front tire traction forces may also be mathematically represented as a single lateral force acting through the front axle at its midpoint. This mathematical representation applies even if collision forces laterally redistribute the loads carried by each tire on an axle.

A free body diagram of the forces acting on the surface vehicle is illustrated in Figure 2.

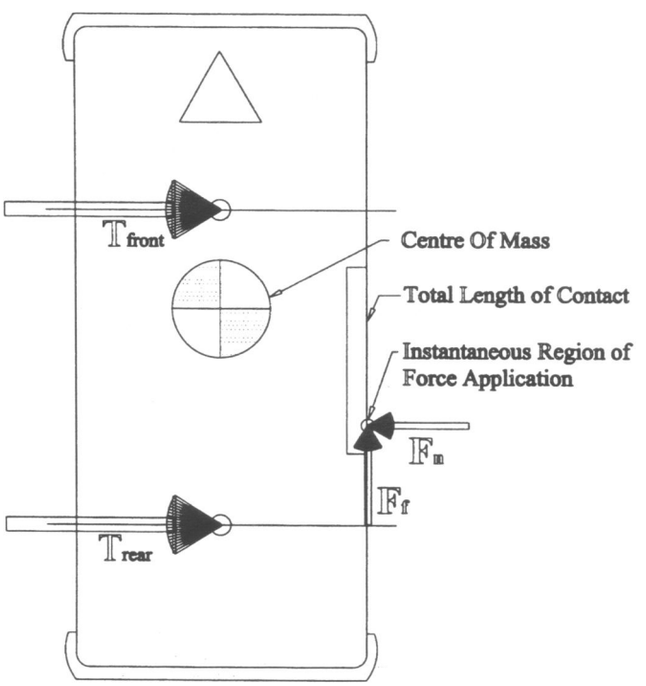

Figure 2. Forces Acting on the Surface Vehicle

The maximum tire forces ($T_{front\text{-}max}$ and $T_{rear\text{-}max}$, respectively) generated by the front and rear pairs of tires are dependent upon the tire/roadway coefficient of friction (μ_T) and the mass (m_{front} and m_{rear} , respectively) supported by each pair of tires. These maximum traction values are approximated as:

$$T_{front-max} = \mu_T m_{front} g \quad (13)$$

$$T_{rear-max} = \mu_T m_{rear} g \quad (14)$$

where: g = gravitational constant (9.81 m/s^2)

Lateral Tire Displacement – Figure 3 illustrates the instantaneous forces acting on the surface vehicle during a sideswipe collision. Lateral acceleration occurs when the applied contact forces exceed the available tire traction. Depending on the magnitude and location of force application, the available traction at either pair of tires may be exceeded. If only one of the vehicle's axles is displaced laterally, then the vehicle will tend to rotate about a point on the other axle. This vehicular motion was observed in the conducted impact tests.

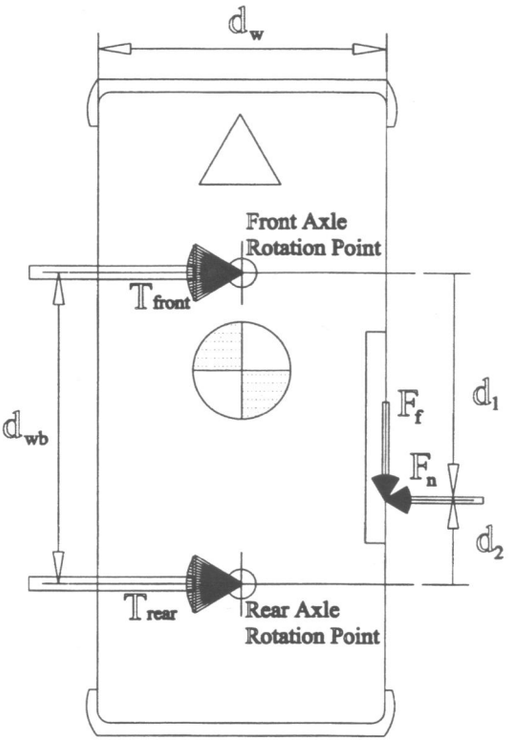

Figure 3. Surface Vehicle Nomenclature

The criteria for slippage of a pair of tires is defined by calculating the moments about the rotation point on the opposing axle. Applying the nomenclature defined in Figure 3, the equations for the moment about the front (M_{front}) and rear (M_{rear}) axles for an instantaneous point during the collision are given by:

$$M_{front} = F_n d_1 + \frac{1}{2} F_f d_w - T_{rear} d_{wb} \quad (15)$$

$$M_{rear} = F_n d_2 - \frac{1}{2} F_f d_w - T_{front} d_{wb} \quad (16)$$

where: d_1 = distance rearward from the front axle to the contact point

d_2 = distance forward from the rear axle to the contact point

d_{wb} = vehicle wheel base

d_w = vehicle width

T_{front}, T_{rear} = tire traction forces

F_n = normal force

F_f = friction force, positive value if acting rearward and negative value if acting forward

In equations 15 and 16, the moment must be less than or equal to zero in order to maintain static equilibrium; a positive net moment will result in rotational acceleration. These equations can be solved in order to determine where the contact forces must be applied to the surface vehicle for rotation to occur about the front or rear axle. Equation 15 is utilized to assess the minimum distance (d_f) rearward of the front axle where the applied forces will exceed the maximum available rear tire traction ($T_{rear\text{-}max}$) and produce rotation about the front axle. This calculation is accomplished by considering that the onset of rotation occurs when the sum of all moments is zero; thus, this boundary is established by defining the net moment (M_{front}) to be zero and solving equation 15 for d_f (i.e. d_1). Lateral displacement of the rear tires will occur for all points of force application rearward of d_f.

Applying these substitutions and solving equation 15 for d_f yields the proximal boundary of the rear tires' slippage zone:

$$F_n d_f + \frac{1}{2} F_f d_w - T_{rear-max} d_{wb} = 0 \quad (17)$$

$$d_f = \frac{-\frac{1}{2} F_f d_w + T_{rear-max} d_{wb}}{F_n} \quad (18)$$

where: F_f is positive if acting rearward and negative if acting forward

Thus, when the contact forces are applied rearward of the front axle by a distance of d_f or more, the rear tires will slide laterally as the vehicle rotates about the front axle.

Applying similar substitutions and solving equation 16 for d_2 yields the proximal boundary (d_r) of the front tires' slippage zone. Thus, d_r is given by equation 20. Similarly, when the applied contact forces act forward of the rear axle by a distance of d_r or more, the front tires will slide laterally as the vehicle rotates about the rear axle.

$$F_n d_r - \frac{1}{2} F_f d_w - T_{front-max} d_{wb} = 0 \quad (19)$$

$$d_r = \frac{\frac{1}{2} F_f d_w + T_{front-max} d_{wb}}{F_n} \quad (20)$$

where: F_f is positive if acting rearward and negative if acting forward

Lateral Slip Regions – Superimposing the evaluated zones of tire slippage on the geometry of the surface vehicle defines which portions of the contact length would permit tire slippage (i.e. vehicle rotation) when the considered contact force is applied. If the front and rear tire slippage zones overlap, then there exists a region where both pairs of tires may simultaneously slip. If applicable, each of these three regions must be considered independently. If the front and rear slip zones do not overlap, then the portion of the sideswipe in the intermediate zone (between d_f and d_r) is unable to overcome the tire traction and no lateral motion occurs. If the contacted area on the surface vehicle does not overlap either of the slip regimes, then no lateral vehicular translation occurs (i.e. the resulting vehicle acceleration is purely longitudinal) and this portion of the analysis may be omitted.

Comparison of the slippage zones with the contacted region on the surface vehicle indicates the modes of lateral tire motion that occur. The length of sliding contact on the surface vehicle must be partitioned according to the portions of its length within each of the lateral tire slip regimes. A representation of this process and definition of related variables are presented in Figure 4. In this analysis, the subscripts "f" and "r" are applied to describe parameters associated with rotation about the front and rear axles, respectively.

Slippage of each pair of tires indicates rotation about the opposing axle. Thus, the distances S_f and S_r are defined as the lengths of contact that produce rotation about only the front axle (subscript "f") and rear axle (subscript "r"), respectively. Slippage of all tires may be conceptualized as simultaneous rotation about both axles; thus, the distance S_{fr} is defined as the length of contact over which rotation simultaneously occurs about both the front and rear axles (subscript "fr"). Depending on the location of the surface vehicle's impacted area and the magnitude of the contact forces, there may be a portion of the contacted area in all, some or none of the three potential rotation zones. The time duration of each rotation mode (t_f, t_{fr} and t_r) may be assessed from the distances S_f, S_{fr} and S_r, respectively, by applying previously evaluated parameters. The closing speed (V_c) at any point during the sliding contact may be assessed from either the initial closing speed ($V_{c\text{-}initial}$) or the final closing speed ($V_{c\text{-}final}$). The previously assessed closing acceleration (a_c) and the distance of the point in question to either the beginning (S_b) or to the end (S_e) of the contact length are

also required. With this knowledge, the closing speed (V_c) at any point may be calculated by applying either equation 21 or 22:

$$V_c = \sqrt{V_{c-initial}^2 - 2 * a_c * s_b} \qquad (21)$$

or

$$V_c = \sqrt{V_{c-final}^2 + 2 * a_c * s_e} \qquad (22)$$

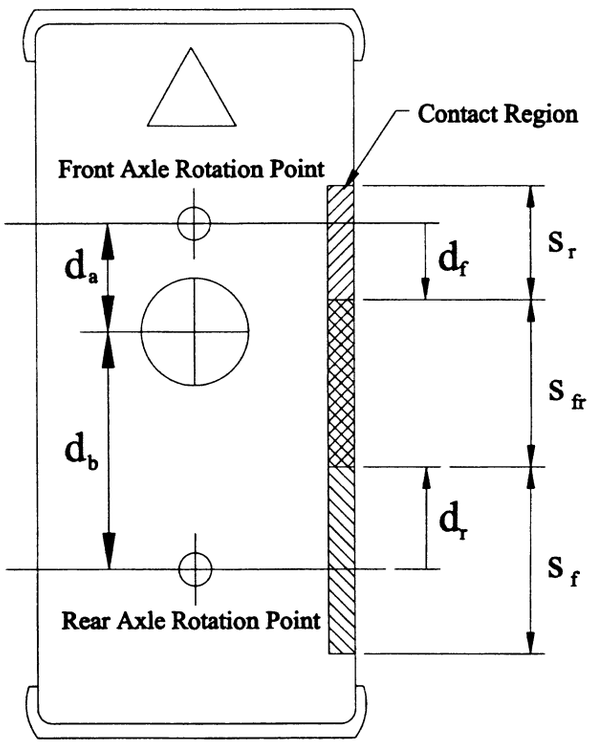

Figure 4. Division of Contact Length into Tire Slip Regions

Equations 21 and 22 are used to calculate the initial and final closing speed values (V_c) for each applicable lateral tire slip zone.

Once the closing speed (V_c) has been calculated for the initiation and completion of sliding motion within each rotation region, the time duration of contact in each zone may be evaluated from:

$$\Delta t = \frac{V_{c-initial} - V_{c-final}}{a_c} \qquad (23)$$

where: $\Delta t = \Delta t_r$ for contact zone s_r

Δt_{fr} for contact zone s_{fr}

Δt_f for contact zone s_f

$V_{c-initial}$ and $V_{c-final}$ = closing speed at initiation and completion of sliding travel in respective contact zones s_r, s_{fr} or s_f

Rotation About Front Axle – In order to assess the lateral speed change for the region of contact where the surface vehicle's rear tires are displaced laterally, the average moment acting about the front axle must be determined. The average moment arm length ($\overline{S}_f$) defines the distance from the axis of rotation to the mid-point of S_f. The average moment ($\overline{M}_f$) may be assessed from this average moment arm length ($\overline{S}_f$) by substituting $\overline{S}_f$ in place of term d_1 in equation 15 and solving for $\overline{M}_f$. The rotational acceleration rate (ω_f) about the front axle is then given by :

$$\omega_f = \frac{\overline{M}_f}{I_{f-yaw}} \Delta t_f \qquad (24)$$

The mass moment of inertia in yaw (I_{f-yaw}) applied in equation 24 may be obtained from published values of the mass moment of inertia about the vehicle's center of gravity (I_{CG}) and a factor defined by the parallel axis theorem to apply this value to rotation about the front axle rotation point (from figure 4, the distance from the center of gravity to the axle rotation point is d_a):

$$I_{f-yaw} = I_{CG} + m_A d_a^2 \qquad (25)$$

The rotational speed change of the center of mass from rotation about the front axle is calculated by multiplying the distance from the center of rotation to the vehicle center of mass (d_a) by the angular velocity at the end of the rotation period. For minimal rotation angles, the direction of the rotational speed change about the front axle for the surface vehicle is approximately lateral and the rotational speed change may be approximated as a lateral speed change (ΔV_{A-f}):

$$\Delta V_{A-f} = \omega_f d_a \qquad (26)$$

Rotation About Rear Axle – An identical procedure is followed to assess displacement of the front tires and rotation about the rear axle. $\overline{S}_r$ is defined as the distance from the rear axle to the mid-point of the region S_r. The average moment acting about the rear axle ($\overline{M}_r$) is determined by substituting $\overline{S}_r$ for the term d_2 in equation 16. For rotation about the rear axle, the mass moment of inertia in yaw (I_{r-yaw}) is given by:

$$I_{r-yaw} = I_{CG} + m_A d_b^2 \qquad (27)$$

where: d_b = distance from rear rotation point to center of gravity

The angular velocity about the rear axle (ω_r) is then defined from equation 24 with the updated variables. For minor vehicle rotation angles, the rotational speed change about the rear axle for the surface vehicle may be approximated as a lateral speed change (ΔV_{A-r}) of:

$$\Delta V_{A-r} = \omega_r d_b \qquad (28)$$

Lateral Translation – In the regime where all tires slip laterally, the surface vehicle's center of mass primarily accelerates laterally.

The surface vehicle is modeled as a rigid body such that body motion on the vehicle's suspension and lateral flexing of the tire sidewalls are ignored. Therefore, for lateral translation to occur, the contact forces are required to overcome tire traction. The net lateral acceleration ($a_{A\,lat}$) of the vehicle's center of mass is evaluated by calculating the difference between the lateral contact (F_n) and maximum tire traction ($T_{front\text{-}max}$ and $T_{rear\text{-}max}$) forces, and dividing by the vehicle's mass (m_A). A positive value for the net lateral acceleration is required for lateral acceleration to occur.

$$a_{A\text{-}lat} = \frac{F_n - T_{front\text{-}max} - T_{rear\text{-}max}}{m_A} \quad (29)$$

The corresponding lateral speed change ($\Delta V_{A\text{-}fr}$) during this phase of contact may then be evaluated by:

$$\Delta V_{A\text{-}fr} = a_{A\text{-}lat}\,\Delta t_{fr} \quad (30)$$

TOTAL SPEED CHANGES – Finally, the total speed change ΔV_A for the surface vehicle is defined by performing the vectorial addition of the contributing speed change components in the longitudinal and lateral directions:

$$\Delta V_A = \sqrt{\left(\Delta V_{A\text{-}fr} + \Delta V_{A\text{-}f} + \Delta V_{A\text{-}r}\right)^2 + \Delta V_{A\text{-}long}{}^2} \quad (31)$$

The effective average acceleration rate acting over the collision event may be represented as:

$$a_{A\text{-}avg} = \frac{\Delta V_A}{\Delta t} \quad (32)$$

The described analytical method involves the evaluation of contact forces acting on the surface vehicle. Identically opposing normal and frictional contact forces act on the contact vehicle; however, the acceleration effect of these forces on the contact vehicle is dependent upon the location of the applied forces on the contact vehicle and its relative angle. Thus, the contact vehicle speed change may be evaluated by adapting this outlined analytical sequence to the contact vehicle.

SPECIAL CONSIDERATIONS FOR ANALYSIS OF SIDESWIPE COLLISIONS – The proposed analytical method assumes that the longitudinal tire forces of the surface vehicle are negligible. If the vehicle is being braked or accelerated, then the longitudinal tire forces would not be negligible and must be considered.

This analytical method may be applied to most sideswipe contacts. However, if two vehicles become parallel such that they are both surface vehicles and there is no distinct contact vehicle, then great caution must be taken in designating one vehicle as the contact vehicle. Generally, in such cases both vehicles will have a series of abrasions along the side panels and it will be difficult to select a representative contact length (C).

Finally, the intended scope of this analytical model was defined earlier in this paper. Applications of this procedure beyond its defined limits requires that proper and complete consideration is given to all additional factors.

IMPACT TESTS

A series of sideswipe collisions were staged; the measured vehicle speed changes were compared to the values yielded by the proposed analytical model. While these tests provide an understanding of the model's validity, these tests are not intended to substitute for a rigorous validation. More rigorous testing is necessary to fully validate the proposed analysis procedure and establish meaningful error bounds.

EQUIPMENT AND PROCEDURES – Test vehicles were acquired and used to conduct several series of vehicle-to-barrier and vehicle-to-vehicle sideswipe collisions. The experimental vehicles were not modified prior to the testing.

Vehicle-to-Barrier Configuration – An "immovable" barrier was constructed of four concrete blocks which interlock to form a 1.5 x 1.5 x 1.5 m cube with a combined mass of approximately 8000kg. A detached automobile trunk lid was secured around one corner of the barrier. The trunk lid provided a representative sample of painted auto body sheet metal (i.e. a contact vehicle). Figure 5 illustrates the trunk lid concrete barrier assembly.

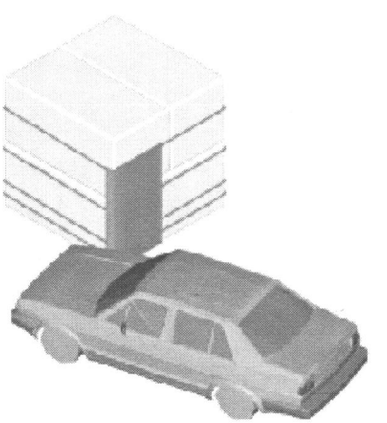

Figure 5. Barrier Configuration

In these tests, the surface vehicle was rolled (forward or reverse) toward the trunk lid. As the surface vehicle approached the barrier, the operator steered the vehicle such that its fenders, doors, and/or quarter panels slid against the anchored trunk lid until the vehicle stopped. This test configuration simulated sliding contact between the side panels of two vehicles.

Vehicle-to-Vehicle Configuration – The second type of sideswipe test was configured by parking the contact vehicle alongside the concrete barrier. Lateral motion of this vehicle was prevented by compressing a spacer block between the vehicle's tires and the concrete barrier; this support inertially anchored the vehicle's suspension to the barrier. Figure 6 illustrates the test geometry for the vehicle-to-vehicle collisions.

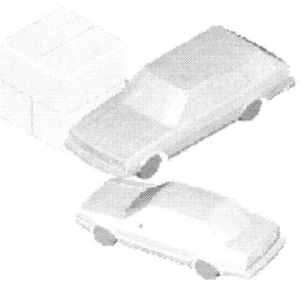

Figure 6. Vehicle-to-Vehicle Configuration

In these tests, the surface vehicle was rolled forward toward the corner of the contact vehicle. The operator steered the vehicle such that its side panels contacted and slid along the left corner of the contact vehicle's front bumper until the surface vehicle came to a stop. This test configuration simulated bumper-to-body panel sliding contact.

Data Acquisition – The impact speed and the collision speed-time history were recorded using a "Stalker" radar gun. The radar gun was calibrated prior to each test series; no functionality faults were recorded. The radar gun unit was linked to a computer via a serial port connection; speed values were sampled at a rate of 31.25 Hz to a precision of 0.1 km/h. The data acquisition was controlled through proprietary software .

An INTECH 5th wheel was also mounted on the moving surface vehicle in some of the tests to supplement the radar data. A tethered portable computer sampled and recorded position / time data for the surface vehicle from an optical encoder on the 5th wheel. The instantaneous velocity of the surface vehicle was calculated from the 5th wheel data by differentiating the distance traveled with respect to time. The optical encoder used has a resolution of 8192 pulses per revolution which corresponds to a traveled distance of 0.26 mm per pulse. Consequently, this resolution corresponds to an idealized positional accuracy of +/- 0.13 mm. The 5th wheel system is capable of an acquisition rate of up to 200 Hz.

Documentation of Vehicular Damage – The staged collisions were documented using two fixed video cameras that were positioned to provide an overview and top view of the contacted regions on the involved vehicle(s). The damage sustained by the surface vehicle was documented after each test. If the damaged regions of the surface vehicle overlapped, the new contact damage produced by a test was resolved from previous damage.

In examining the surface vehicle, the primary purpose is to record the total length of sliding contact including those regions where only threshold deformation and abrasions are present. Figure 7 illustrates a typical damage pattern on a surface vehicle. Evidence of wheel contact and snagging should also be documented, although they are to be evaluated independently of the sideswipe.

Figure 7. Sliding Contact Damage to a Surface Vehicle.

In examining the contact vehicle (or the barrier mounted trunk lid), the purpose is to identify and document the area that made sliding contact with the surface vehicle. This contact region is referred to as the "contact patch". Evidence such as scuff marks, deep abrasions and material deposits characterize the contact patch. There is often a region adjoining the contact patch where the road grime has been cleaned and/or very minor abrasions are present. This peripheral area does not reflect a region where significant force has been transmitted and is not considered to be a part of the contact patch. Figure 8 illustrates a contact patch.

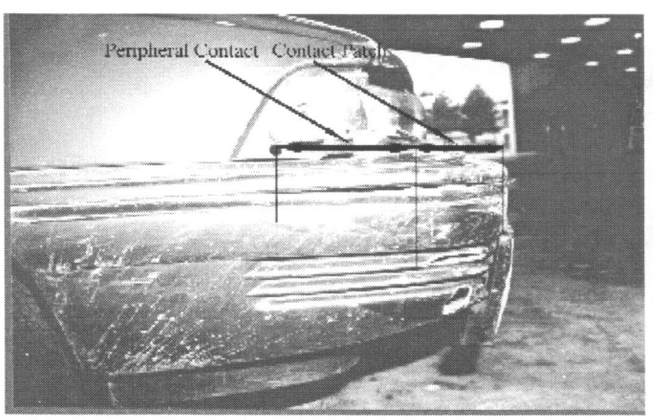

Figure 8. Sliding Contact Damage to a Contact Vehicle.

FORD LTD TESTS – A series of six vehicle-to-barrier tests were conducted using a 1984 Ford LTD sedan as the surface vehicle; these experiments were conducted to develop and refine the sideswipe testing procedure.

FORD FAIRMONT VEHICLE-TO-BARRIER TESTS – A series of tests were conducted using a 1978 Ford Fairmont in the vehicle-to-barrier impact configuration. A Mazda Miata Trunk lid was secured to the barrier as the "contact" surface.

Both the left and right sides of the Ford Fairmont amassed sliding contact type damage over the majority of their lengths during this test series. This damage consisted of sliding horizontal abrasions with smeared deposits of transferred paint. Shallow (<2.5 cm) deformation and threshold damage were present on some of the body skin contact areas. Threshold damage refers to the onset of residual deformation; the depth of threshold deformation is immeasurable. Some of the prominences on the vehicle's side panels (e.g. wheel well perimeter trim) were shifted in the direction of their respective contacts.

The Mazda Miata trunk lid surface was reshaped by the cumulative effect of multiple impacts. Successive impacts flattened the lid's contact surfaces and produced creases. In the latter tests, the crease prominences on the trunk lid recorded evidence of contact while the indented surfaces were untouched. An effective contact patch was estimated for these tests from the sum of the areas within the contact patch that exhibited evidence of direct contact; an effective average contact patch width of about 13 cm (5") was applied to the affected vehicle-to-barrier sideswipe impact tests.

Four tests were rejected from the data set. Tests Fair04R and Fair10L were not included because notable snagging had occurred. Tests Fair12L and Fair14L were also not included because the initial vehicle speed was not completely dissipated by frictional contact; consequently, the vehicle speed changes during these tests were unknown. In all other tests, the test vehicle came to a stop at the end of sliding contact.

The analysis of the Ford Fairmont test data considered stiffness coefficients from NHTSA[5] and Prasad[6], [7]. Although an identical vehicle was not tested by Prasad, the stiffness values for a 1980 Ford LTD were adopted as the manufacturer, vintage and body size were similar to the tested vehicle. The applied NHTSA stiffness data were default values from the class 3 category; the Ford Fairmont is specified as a class 3 vehicle. The applied coefficients are summarized in Table 1.

Table 1. Fairmont Stiffness Data

	Ford Fairmont
Prasad	A=237.8 lb/in B=62.9 lb/in^2 (1980 Ford LTD)
NHTSA	A=173 lb/in B=57lb/in^2 (Default Class Ford Fairmont, Class3)

The test results and the analysis of the Fairmont testing using the Prasad and NHTSA values (from Table 1) are presented in Table 2.

MAZDA GLC AND CHEVROLET CHEVETTE VEHICLE-TO-BARRIER TESTING – A series of vehicle-to-barrier tests were conducted using a 1981 Mazda GLC 2-door hatchback and a 1979 Chevrolet Chevette 4 door hatchback. A Pontiac Sunfire trunk lid was used as the barrier mounted collision surface. Impacts were conducted by sliding the right side of each vehicle forward along the barrier.

The analysis of the GLC and Chevette test data utilized Prasad and NHTSA stiffness coefficients. Although identical vehicles were not tested by Prasad, the stiffness values for a 1980 Chevrolet Citation and a 1983 Mazda 626 were considered to be representative as the manufacturers , vintages and body sizes were similar to the tested vehicles. The applied coefficients are presented in Table 3.

Results from the analysis of the GLC and Chevette tests using the Prasad and NHTSA values (from Table 3) are summarized in Table 4. Test Chev01R was discarded because direct contact with the concrete barrier occurred.

Table 2. Ford Fairmont Tests and Analysis Results

Test	Vehicle's Approach Direction	Speed Change [km/h]	Calculated Impact Speed/ Speed Change [km/h]		Description of Damage and Comments
			Prasad	NHTSA	
Fair01R*	Forward	4.2	3.1	2.7	Minor tire contact, side trim compressed.
Fair02R	Forward	6.1	7.8	6.4	Fender: buckled, abraded.
Fair03R	Forward	6.3	7.5	6.4	Front right door: abrasive contact shallow deformation.
Fair04R	Forward	7.7			Front right door snag: door hinge deformed rearward.
Fair05R	Forward	8.2	10.0	8.3	Extended sliding contact on right side doors and fender.
Fair06L	Rearward	4.1	2.3	2.0	Threshold deformation to middle of the operator's door.
Fair07L	Rearward	4.5	7.9	6.7	Minor deformation and paint transfer to operator's door.
Fair08L	Rearward	5.2	5.6	4.8	Deformation of the operator's door.
Fair09L	Rearward	5.1	7.7	6.5	Threshold damage on the rear left door.
Fair10L	Forward	6.8			Front left tire directly contacted concrete barrier.
Fair11L	Forward	8.0	11.3	8.1	Minor rear left door damage.
Fair12L	Forward	9.0			Barrier contact did not stop the vehicle.
Fair13L	Forward	8.7	10.9	7.9	Surface deformation from the rear left door to the rear left wheel well.
Fair14L	Forward	9.7			Contact across left doors. Barrier contact did not stop the vehicle.
Fair15L	Forward	9.6	11.9	8.9	Deformation to left doors.
Average Difference			1.5	-0.1	
Standard Deviation			1.7	1.2	

* The suffix "R" designates impacts to the right side of the vehicle while "L" designates impacts to the left side.

Table 3. Chevette and GLC Stiffness Data

	Chevrolet Chevette	Mazda GLC
Prasad	A=175.4 lb/in B=34.2 lb/in^2 (1980 Chevrolet Citation)	A=165.1 lb/in B=30.3 lb/in^2 (1983 Mazda 626)
NHTSA	A=140 lb/in B=67.0 lb/in^2 (Chevrolet Chevette, Class 2)	A=77.0 lb/in B=37.0 lb/in^2 (Mazda GLC, Class 1)

MAZDA GLC AND CHEVROLET CHEVETTE VEHICLE-TO-VEHICLE TESTING – The Mazda GLC and Chevrolet Chevette were also utilized in a series of vehicle-to-vehicle tests. In each test, the surface vehicle was rolled rearward resulting in the left side paneling sliding along the left corner of the contact vehicle's front bumper. These tests and the corresponding analytical results are summarized in Table 5. The speed change was assessed using the proposed algorithm and the stiffness coefficients presented in Table 3.

Table 4. Chevette and GLC Vehicle-to-Barrier Tests and Analysis Results

Test	Vehicle's Approach Direction	Speed Change [km/h]	Calculated Speed Change [km/h]		Description of Damage and Comments
			Prasad	NHTSA	
GLC03R	Forward	6.6	6.1	4.1	Right door: threshold contact.
GLC04R	Forward	5.3	4.8	3.2	Right door: threshold contact.
CHEV01R	Forward	6.0			Front right wheel well lip contacted concrete barrier directly.
CHEV02R	Forward	6.8	5.4	4.8	Right door: shallow deformation.
Average Difference			-0.8	-2.2	
Standard Deviation			0.5	0.3	

Table 5. Chevette and GLC Vehicle-to-Vehicle Tests and Analysis Results

TestVehicle's Approach DirectionSpeed Change [km/h]			Calculated Impact Speed/Speed Change[km/h]		Description of Damage and Comments
			Prasad	NHTSA	
GLC01L	Rearward	8.8	8.7	6.0	Rear left wheel hub-cap cracked. Contact to operator's door and left quarter panel.
GLC03L	Rearward	10.1	12.7	9.1	Contact from operator's door to trailing edge of front tire.
CHEV01L	Rearward	7.2	6.8	6.6	Left fender deformation.
CHEV02L	Rearward	7.2	7.5	7.0	Slight snag of front left door.
Average Difference			0.6	-1.2	
Standard Deviation			1.4	1.1	

SUMMARY OF TEST RESULTS – In the conducted tests, the surface vehicle exhibited horizontal abrasions, gouges and paint smears over an extended length while the "contact" trunk lid (vehicle-to-barrier tests) and the bumper cover of the contact vehicle (vehicle-to-vehicle contacts) exhibited marks over a short horizontal distance (i.e. the "contact patch").

The staged sideswipe collisions were characterized by a gradual deceleration from the impact speed to a stopped position; the vehicular rebound and restitution was insignificant in those tests where no snagging occurred. Thus, the total vehicular speed change equated to the recorded impact speed. The impact speed was determined from the radar and/or 5th wheel speed-time data by observing the initiation of deceleration.

SUMMARY OF ANALYTICAL RESULTS – In reviewing the analytical results, caution must be applied when interpreting the predicted values for individual tests since not all motion specific factors were monitored and incorporated in this assessment. Thus, the complete data set was considered when evaluating the validity of the proposed model.

Some of the conducted tests had relatively low speed changes (as low as 4.1 and 4.5 km/h). For such speed changes it is potentially misleading to express the difference between the predicted and measured values in the form of a percentage error. For example, the largest percentage underestimate occurred in applying the NHTSA stiffness coefficients to the test Fair06L, where an underestimate of 51% resulted; however, in a more meaningful context, the model underestimated the measured value by 2.1 km/h. Similarly, the largest percentage error emerged in test Fair07L, where the analytical model overestimated the measured speed by 3.4 km/h (76%) for the Prasad data and 2.2 km/h (49%) for the NHTSA data.

It was observed that comparable absolute differences occurred across the spectrum of tested speed changes; this resulted in percentage error that decreased with increasing speed change. As the absolute differences remained relatively independent across the tested range, the accuracy and precision of the analytical results are discussed within the context of average difference and standard deviation.

Fairmont Tests – The average difference between the actual impact speed and the calculated impact speed was +1.5 km/h with a standard deviation of 1.7 km/h when the Prasad data was utilized. An average difference of -0.1 km/h and a standard deviation of 1.2 km/h were recorded when the NHTSA data was utilized.

GLC and Chevette Tests – The analysis of the GLC and Chevette tests that utilized the Prasad coefficients had an average difference between the actual impact speed and the calculated impact speed of less than 0.01 km/h with a standard deviation of 1.3 km/h. The analysis utilizing the NHTSA coefficients resulted in an average difference of -1.6 km/h with a standard deviation of 1.0 km/h.

Total Test Data – Combining all of the evaluated tests, an average overestimate of 0.9 km/h and a standard deviation of 1.3 km/h were recorded when applying Prasad data to the proposed algorithm. When using NHTSA stiffness coefficient values, the proposed algorithm yielded an average underestimate of 0.7 km/h with a standard deviation of 1.6 km/h.

The results yielded from application of the Prasad and NHTSA coefficients to the conducted tests do not preferentially support one source of stiffness data over another. In cases where the vehicle model year is sufficiently later than the source data used to compare the NHTSA values, it is logical to not consider NHTSA default A and B values in favor of more recent data. Otherwise, unless vehicle specific data are available, it is advised to consider both sources to yield a range.

The observed consistency between the calculated and recorded impact speeds suggests that the proposed algorithm models sideswipe collisions reasonably; however, the same tests also indicate that there is an inherent variance between the calculated value and the measured value. The conducted tests provide an understanding about the validity of this model and the accuracy of the available stiffness data for only three vehicle types in a total of 18 contacts. This limited experimentation is insufficient to globally quantify the confidence limits of the predictive model. However, comparison of the analytical and actual speed change values suggests that the model is valid.

LIMITATIONS OF ANALYSIS PROCEDURE – There are several factors which define the accuracy of this analysis procedure. Most influential is the accuracy of the applied stiffness data. The published A and B values are derived from staged high speed collisions. While the conducted tests presented in this paper suggest a correlation between the calculated values (using these A and B coefficients) and the test speed changes, there is inherent variability resulting from the application of these coefficients to sideswipe collisions where limited or no residual crush is present. Furthermore, when vehicle specific stiffness data are not available, the selection of appropriate stiffness values requires justifiable consideration. Thus, the availability of vehicle specific stiffness data for intended application to minimal crush contacts is a current limitation to the accuracy of this procedure; however, this variation may be minimized with prudent selection of stiffness values from the data that is available.

The interpretation of vehicular damage also has the potential to influence the accuracy of the results. In the Crash 3 vehicle stiffness model, the contact force per unit length may be up to the value of "A" without crushing the vehicle surface. In the proposed model, the normal force acting on contact regions that were not crushed is assumed to be at the threshold of deformation. This assumption represents a maximum estimate of the contact force which may result in an overestimate of the collision speed change in those cases where a significant amount of sub-threshold contact is present.

A similar caution relates to the interpretation of the contact patch length on the contact vehicle. The contacted area of the contact vehicle may include a peripheral region which exhibits evidence of contact but minimal force transmission. Although this peripheral region should be excluded from the contact patch length, the smooth transition between these two areas tends to obscure their distinction. Furthermore, it should be recognized that not all of the contact patch necessarily was in complete contact with the surface vehicle for the entire duration of the sideswipe; as the collision progressed, an evolving relative collision geometry may have slightly advanced the contact patch on the contact vehicle. However, careful examination of the contact patch will assist the analyst in choosing a meaningful contact patch length.

As a consequence of these factors, there is a natural variation in the results of the predictive model. However, the tests presented in this paper illustrate that the predicted speed change was relatively consistent with the recorded value. Thus, this limited validation demonstrates that the analytical technique fits the model well, although local variations are to be expected. These variations may be minimized with a comprehensive examination of the damage and proper consideration of all relevant factors.

CONCLUSIONS

Sideswipe collisions differ from conventional "impacts"; unlike traditional impacts, the contacting vehicular surfaces do not necessarily achieve a common velocity during sideswipe contacts. Currently, no other practical procedures for analyzing the sideswipe exist. This paper presents an analytical model that may be practically applied to the analysis of sideswipe collisions. By utilizing available empirical data, the proposed sideswipe analysis model permits evaluation of vehicle speed changes, accelerations, and the collision duration from measurements of vehicular damage.

Several series of sideswipe contact tests were conducted. The proposed analysis technique was applied to the test data using representative vehicle stiffness values from Prasad and NHTSA. This limited validation yielded that this analytical procedure models sideswipe collisions well, although local variations are to be expected.

RECOMMENDATIONS

Testing to refine representative vehicle-to-vehicle coefficients of friction and additional empirical vehicle side stiffness data would permit application of the analytical procedure with greater precision. Further experimentation is recommended to validate the proposed analytical model and define a representative confidence interval.

ACKNOWLEDGMENT

This project would not have been possible without the efforts of the entire INTECH Engineering staff. In particular, the authors are appreciative of the assistance from Angela Giroux.

REFERENCES

1. Bailey, M.N., Wong, B.C., Lawrence, J.M., "Data and Methods for Estimating the Severity of Minor Impacts," 950352, Society of Automotive Engineers, Inc., Warrendale, PA, 1995.
2. Griffin, M.J., "Evaluation of Vibration with Respect to Human Response," 860047, Society of Automotive Engineers, Inc., Warrendale, PA, 1986.
3. Warner, C.Y., Smith, G.C., James, M.B., Germane, G.J., "Friction Applications in Accident Reconstruction," 830612, Society of Automotive Engineers, Inc., Warrendale, PA, 1983.
4. Emori, R.I. "Analytical Approach to Automobile Collisions," 680016, Society of Automotive Engineers, Inc., Warrendale, PA, 1968.
5. Tsongos, N.G. (CRASH Program Manager), "Crash 3 Technical Manual" U.S. Government Printing Office, 1986.
6. Prasad, A.K. "CRASH3 Damage Algorithm Reformulation for Front and Rear Collisions," 900098, Society of Automotive Engineers, Inc., Warrendale, PA, 1990.
7. Prasad, A.K. "Energy Absorbed by Vehicle Structures in Side-Impacts," 910599, Society of Automotive Engineers, Inc., Warrendale, PA, 1991.

ABOUT THE MAIN AUTHOR

Amrit Toor, Ph.D., is employed as a mechanical engineer specializing in accident reconstruction services at INTECH Engineering in Vancouver, British Columbia, Canada.

Questions or comments on the paper are welcomed and can be forwarded to:

INTECH Engineering Ltd.
#24 - 7711 - 128th Street
Surrey, BC V3W 4E6

Phone: (604) 572-9900
Fax: (604) 572-9901
http://www.intech-eng.com
e-mail: intech@intech-eng.com

APPENDIX A: WORKED EXAMPLE

This example considers a scenario involving vehicles A and B. Vehicle B is stopped at an intersection and is just about to start accelerating forward. Vehicle A passes the L side of vehicle B and the right side of vehicle A slides along the front left corner of vehicle B.

Figure A1 illustrates the orientation of the surface (A) and contact (B) vehicles during the collision. The surface vehicle was oriented at the indicated angle (α) of 45°.

The purpose of this analysis is to assess the maximum speed change sustained by the surface vehicle. The following information is available from examination of the involved vehicles.

Surface Vehicle:

- 1981 Ford Granada - 2 door Coupe
- Contact initiates 4.93m (194") from the rear right corner and extends across the right fender, doors, and quarter panel. The contact ends at 0.74 m (29") from the rear right corner. The total contact length is 4.19m (165")
- Average crush depth along contact length : 2.5 cm (1")
- Damage consists of horizontal abrasions and deformation.
- No snagging is observed.

Contact Vehicle:

- 1985 Chevrolet Celebrity - 4 door sedan
- Abrasions and gouges observed on the left corner of the front bumper with a width of contact (C) measured to be 13 cm (5")

The following relevant data were obtained for the involved vehicles†:

Surface Vehicle

- Mass:1275 kg (2810 lb)

† Expert Autostats :
"Expert Autostats 3.6," Forensic Expert Software, LaMesa, CA, USA.

- Curb weight distribution: 55 / 45 % (Front / Rear)
- Total length: 4.98 m (196")
- Wheelbase: 2.67m (105")
- Rear overhang: 1.27m (50")
- Front overhang: 1.04 m (41")
- Maximum width: 1.80 m (71")
- Centre of gravity: 1.47 m (57.8") in front of rear axle and 1.20 m (47.3") behind front axle
- Yaw moment of inertia about centre of gravity: 2289.3 N-m-s^2 (1688.3 lb-ft-s^2)

Contact Vehicle

- Mass:1226 kg (2702 lb)
- Curb weight distribution: 64 / 36 % (Front / Rear)
- Total length: 4.78 m (188")
- Wheelbase: 2.67m (105")
- Rear overhang: 1.02m (40")
- Front overhang: 1.09 m (43")
- Maximum width: 1.75 m (69")
- Centre of gravity: 1.71 m (67.2") in front of rear axle
- Yaw moment of inertia about centre of gravity: 2138.5 N-m-s^2 (1577.1 lb-ft-s^2)

The published side stiffness coefficients for the surface vehicle were obtained from Prasad: A= 34.9 kN/m (199.2 lb/in) and B= 304.1 kN/m^2 (44.1 lb / in^2). These coefficients were utilized to assess the normal force acting on the surface vehicle:

$$F_n = C(A + Bx) = 5411 \text{ N } (1217 \text{ lb})$$

$$F_f = \mu_v F_n = 3247 \text{ N } (730 \text{ lb})$$

$$\text{where: } \mu_V = 0.6$$

$$a_{A-long} = \frac{F_f}{m_A} = 2.5 \text{ m/s}^2 \ (0.26g)$$

In order to assess $a_{B\text{-}long}$ for the contact vehicle, the contact forces must be resolved into components aligned with the axes of the contact vehicle. Figure A2 illustrates the contact forces and relative vehicle axes.

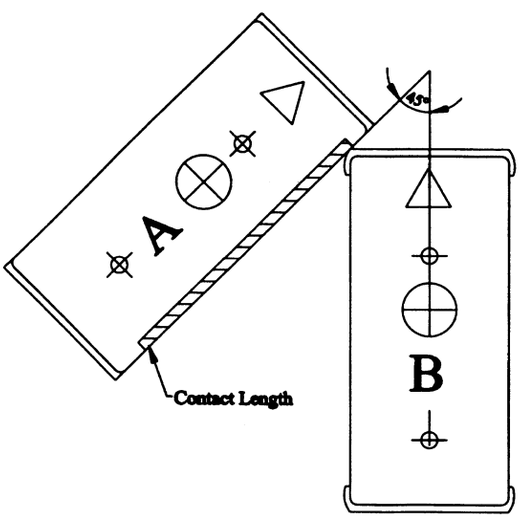

Figure A1: Vehicle Orientation

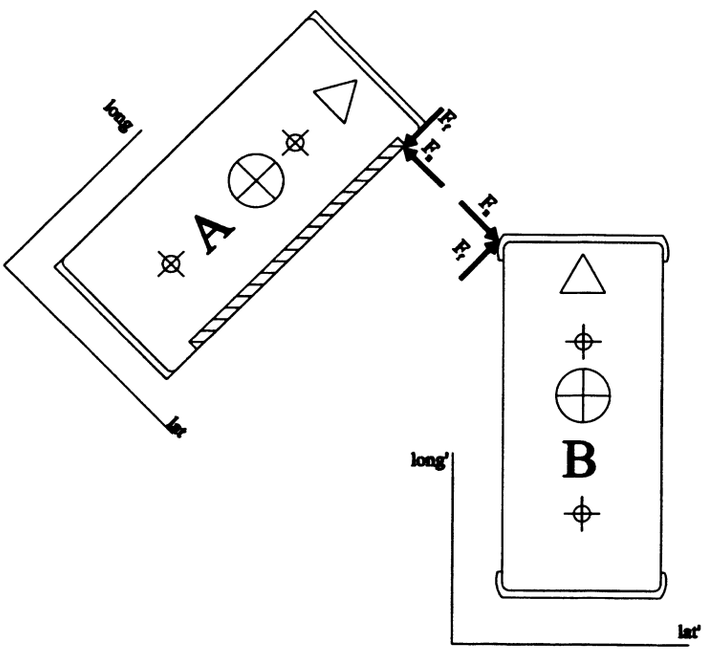

Figure A2: Contact Forces and Relative Vehicle Axes.

The angle between the involved vehicles (α=45°) is utilized to assess the contact force components with respect to the contact vehicle's axes.

$$F_{f-long'} = F_f \cos(\alpha) = 2296 \text{ N (516 lb)}$$
$$F_{f-lat'} = F_f \sin(\alpha) = 2296 \text{ N (516 lb)}$$
$$F_{n-long'} = -F_n \sin(\alpha) = -3826 \text{ N (-860 lb)}$$
$$F_{n-lat'} = F_n \cos(\alpha) = 3826 \text{ N (860 lb)}$$
$$F_{B-long'} = F_{n-long'} + F_{f-long'} = -1530 \text{ N (-344 lb)}$$
$$F_{B-lat'} = F_{n-lat'} + F_{f-lat'} = 6122 \text{ N (1376 lb)}$$

These force components acting on the contact vehicle may cause the vehicle to rotate about the axle furthest from the contacted corner. Therefore, the net moment acting about the rear axle must be assessed. First, the maximum tire traction available at the front and rear pairs of tires is calculated:

$$T_{front-\max(B)} = \mu_T m_{front} g = 5388 \text{ N (1211 lb)}$$
$$T_{rear-\max(B)} = \mu_T m_{rear} g = 3031 \text{ N (681 lb)}$$
where: $\mu_T = 0.7$ (assuming dry asphalt road surface)

The moment is then calculated by utilizing the contact vehicle's wheelbase, front overhang and width.

$$M_{rear} = F_{B-lat'}(d_{wb} + FOH) - \tfrac{1}{2} F_{B-long'} d_w - T_{front-\max(B)} d_{wb}$$
$$M_{rear} = 7294 \text{ N-m (5380 lb-ft)}$$

The lateral acceleration component for the contact vehicle can then be determined from the net moment.

$$I_{r-yaw} = I_{CG} + m_B d_b^2 = 5711 \text{ N}\cdot\text{m}\cdot\text{s}^2 \text{ (4211.7 lb}\cdot\text{ft}\cdot\text{s}^2\text{)}$$
$$\alpha_r = \frac{M_{rear}}{I_{r-yaw}} = 1.28 \text{ rad/s}^2$$
$$a_{B-lat'} = \alpha_r (d_{wb} + FOH) = 4.8 \text{ m/s}^2 \text{ (0.49g)}$$

The longitudinal component of the acceleration is then determined to assess the net acceleration of the front left corner of the contact vehicle.

$$a_{B-long'} = \frac{F_{B-long'}}{m_B} = -1.2 \text{ m/s}^2 \text{ (0.13g)}$$
$$a_{B-total} = \sqrt{a_{B-long'}^2 + a_{B-lat'}^2} = 4.9 \text{ m/s}^2 \text{ (0.50g)}$$
$$\Theta = \arctan\left(\frac{a_{B-long'}}{a_{B-lat'}}\right) = 14.5^\circ$$

The angle θ represents the direction of the net acceleration vector on the contact vehicle expressed in the coordinate system of the contact vehicle. The component of this acceleration along the surface vehicle's longitudinal axis must be assessed in order to determine the closing acceleration rate ($a_{B\text{-long}}$).

$$a_{B-long} = a_{B-total} \sin(90^\circ - \alpha - \Theta) = 2.5 \text{ m/s}^2 \text{ (0.25g)}$$
$$a_c = |a_{A-long}| + |a_{B-long}| = 5.0 \text{ m/s}^2 \text{ (0.51g)}$$

The relative sliding distance can be determined by:

$$D = L - C = 4.06 \text{ m (160")}$$

As the initial and final closing speeds are unknown for this collision scenario, it will be assumed that the vehicles reach a common velocity (ie. $V_{c\text{-final}} = 0$). This assumption yields a maximum contact duration and total speed change.

$$\Delta t_{\max} = \sqrt{\frac{2 * D}{a_c}} = 1.3 \text{ s}$$
$$\Delta V_{A-long} = a_{A-long} \Delta t_{\max} = 3.25 \text{ m/s (10.7ft/sec)}$$
$$= 11.7 \text{ km/h (7.3mph)}$$

The maximum tire traction available for the surface vehicle is:

$$T_{front-\max} = \mu_T m_{front} g = 4815 \text{ N (1083 lb)}$$
$$T_{rear-\max} = \mu_T m_{rear} g = 3940 \text{ N (886 lb)}$$

The lateral tire slip regions are defined by d_f and d_r :

$$d_f = \frac{-\tfrac{1}{2} F_f d_w + T_{rear-\max} d_{wb}}{F_n} = 1.40 \text{ m (55.1")}$$

$$d_r = \frac{\tfrac{1}{2} F_f d_w + T_{front-\max} d_{wb}}{F_n} = 2.92 \text{ m (115")}$$

By superimposing these values on the contact vehicle's geometry, Figure A3 illustrates that the front and rear tire slip regions do not overlap. When the contact forces act within the intermediate contacted area, no lateral motion of the surface vehicle occurs.

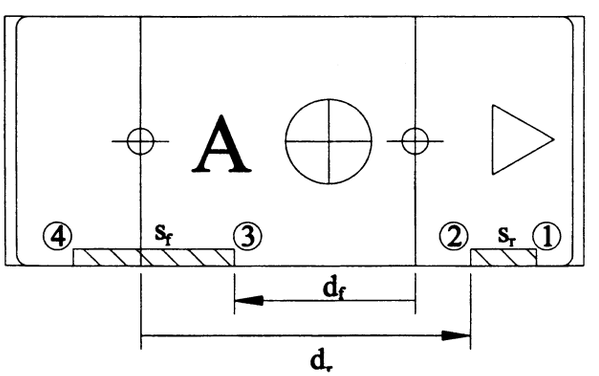

Figure A3: Lateral Slip Regions

The lengths of the two slip regions are assessed from the measured length of contact and the calculated d_f and d_r:

$$s_r = 0.74 \text{ m } (29")$$
$$s_f = 1.80 \text{ m } (71")$$

For convenience, the ends of the regions S_r and S_f have been labelled as points #1 to 4. The closing speeds at the ends of each slip region are then determined by utilizing the distance (s_e) from the point in question to the end of sliding contact (point 4):

$$V_{c1} = \sqrt{V_{c-final}^2 + 2 * a_c * s_{e1}} = 6.5 \text{ m/s } (21.3 \text{ ft/s})$$
$$V_{c2} = \sqrt{V_{c-final}^2 + 2 * a_c * s_{e2}} = 5.9 \text{ m/s } (19.4 \text{ ft/s})$$
$$V_{c3} = \sqrt{V_{c-final}^2 + 2 * a_c * s_{e3}} = 4.2 \text{ m/s } (13.8 \text{ ft/s})$$
$$V_{c4} = V_{c-final} = 0$$

The time duration of contact in each slip region is determined from the assessed closing speeds.

$$\Delta t_r = \frac{V_{c1} - V_{c2}}{a_c} = 0.12 \text{ s}$$
$$\Delta t_f = \frac{V_{c3} - V_{c4}}{a_c} = 0.84 \text{ s}$$

The distance from the rotation point to median of each slip region is determined from the vehicle measurements and the calculated d_f and d_r:

$$\bar{s}_r = 3.29 \text{ m } (130")$$
$$\bar{s}_f = 2.30 \text{ m } (91")$$

The average moments about both the front and rear axles are then calculated:

$$\bar{M}_r = F_n \bar{s}_r - \tfrac{1}{2} F_f d_w - T_{front-max} d_{wb} = 2024 \text{ N-m } (1493 \text{ lb-ft})$$
$$\bar{M}_f = F_n \bar{s}_f + \tfrac{1}{2} F_f d_w - T_{rear-max} d_{wb} = 4848 \text{ N-m } (3576 \text{ lb-ft})$$

The yaw moment of inertia ($I_{f\text{-}yaw}$ and $I_{r\text{-}yaw}$) is required to assess the final angular velocity (ω):

$$I_{r-yaw} = I_{CG} + m_A d_b^2 = 5032.7 \text{ N} \cdot \text{m} \cdot \text{s}^2 (3711 \text{ lb} \cdot \text{ft} \cdot \text{s}^2)$$
$$I_{f-yaw} = I_{CG} + m_A d_a^2 = 4125.3 \text{ N} \cdot \text{m} \cdot \text{s}^2 (3042 \text{ lb} \cdot \text{ft} \cdot \text{s}^2)$$

$$\omega_r = \frac{\bar{M}_r}{I_{r-yaw}} \Delta t_r = 0.05 \text{ rad/s}$$

$$\omega_f = \frac{\bar{M}_f}{I_{f-yaw}} \Delta t_f = 1.0 \text{ rad/s}$$

Thus, the lateral speed changes can be determined for both slip regions:

$$\Delta V_{A-r} = \omega_r d_b = 0.3 \text{ km/h } (0.2 \text{ mph})$$
$$\Delta V_{A-f} = \omega_f d_a = 4.3 \text{ km/h } (2.7 \text{ mph})$$

Finally, the surface vehicle's total speed change and effective acceleration rate are given by:

$$\Delta V_{A-total} = \sqrt{(\Delta V_{A-r} + \Delta V_{A-f})^2 + \Delta V_{A-long}^2} = 12.6 \text{ km/h } (7.9 \text{ mph})$$

$$a_{A-avg} = \frac{\Delta V_{A-total}}{\Delta t} = 0.27g$$

As this analysis made the assumption that the vehicles attained a common velocity at the end of sliding contact, this value represents the maximum speed change. Therefore, $\Delta V_{A\text{-}total} \leq 12.6$ km/h (7.9 mph).

APPENDIX B: ASSESSMENT OF CONTACT VEHICLE'S $a_{B\text{-}LONG}$

The contact vehicle's acceleration component acting along the longitudinal axis of the surface vehicle ($a_{B\text{-}long}$) is primarily dependent on the orientation of the two vehicles. The two extreme cases where the vehicles are parallel or perpendicular will be presented.

Parallel Case

The parallel scenario occurs when the surface and contact vehicles are travelling parallel or almost parallel to each other. Figure B1 illustrates this scenario.

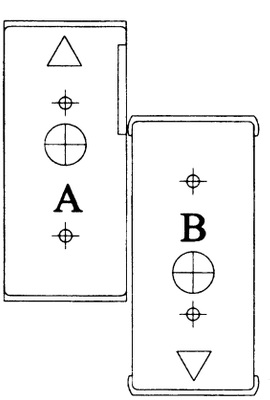

Figure B1: Parallel Travel Paths

Similar to the surface vehicle, the contact vehicle is considered to have free rolling tires. Therefore, as the contact vehicle's longitudinal axis is parallel (or close to parallel) with the longitudinal axis of the surface vehicle, the frictional force (F_f) acting between the vehicles is the only force that accelerates the contact vehicle along its direction of travel. Thus,

$$a_{B-long} = \frac{F_f}{m_B}$$

where m_B = mass of vehicle B

Perpendicular Case

Figure B2 depicts the perpendicular sideswipe collision scenario.

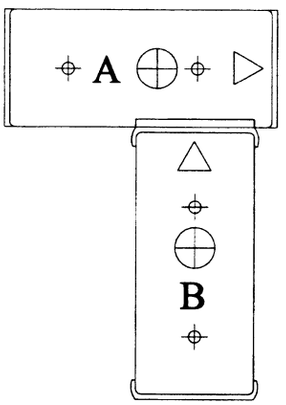

Figure B2: Perpendicular Travel Paths

In this case, the contact vehicle's longitudinal axis is perpendicular to the surface vehicle's longitudinal axis. In order to properly assess the acceleration of the contacted region on the contact vehicle, the effect of tire traction must be considered. If the applied frictional force is sufficient to overcome the available tire traction, then the contact vehicle will accelerate in the surface vehicle's longitudinal direction. If this applied force is insufficient, then the contact vehicle will not accelerate in the longitudinal direction.

The moment must be calculated about the far axle of the contact vehicle:

$$M = F_f(d_{wb} + d) - Td_{wb}$$

where

F_f = frictional force on surface vehicle

d_{wb} = wheelbase of the contact vehicle

d = front overhang on the contact vehicle if the contact vehicle is impacted on the front

= rear overhang on the contact vehicle if the contact vehicle is impacted on the rear

$T = T_{front-max}$ if contact vehicle is impacted on front

$= T_{rear-max}$ if contact vehicle is impacted on rear

If the calculated moment is less than or equal to zero, then the applied contact force is insufficient to overcome the traction and the vehicle will not accelerate laterally. If the calculated moment is greater than zero, then the rotational acceleration is determined by:

$$\alpha = \frac{M}{I_{CG} + m_B d_d^2}$$

where

α = the angular acceleration of the contact vehicle

I_{CG} = moment of inertia of the contact vehicle about its centre of gravity

d_d = d_a if the contact vehicle is impacted on its rear

= d_b if the contact vehicle is impacted on its front

The acceleration of the contact vehicle's contact patch along the longitudinal axis of the surface vehicle is then given by:

$$a_{B-long} = \alpha(d_{wb} + d)$$

Intermediate Cases

The parallel and perpendicular cases define maximum and minimum values for $a_{B\text{-long}}$. If the contact vehicle is oriented at any angle between the two extreme cases, then the normal and frictional forces applied to the vehicle may be resolved into components parallel with the longitudinal and lateral axes of the contact vehicle. The net rotational acceleration may then be evaluated by calculating the moment acting on the far axle of the contact vehicle as in the perpendicular case.